6

A Robust Motion Tracking Control of Piezo-Positioning Mechanism with Hysteresis Estimation

Amir Farrokh Payam,
Mohammad Javad Yazdanpanah and Morteza Fathipour
Department of Electrical and Computer Engineering, University of Tehran, Tehran, Iran

1. Introduction

Piezoelectric actuators are the most suited actuation devices for high precision motion operations in the positioning tasks include miro/nano-positioning [1]. These actuators have unlimited motion resolution and posses some advantages such as ignorable friction, noiseless, zero backlash and easy maintenance, in comparison with the conventional actuated systems which are based on the sliding or revolute lower pairs [2].

Producing large forces, fast response and high efficiency are major advantages of piezoelectric actuators. But, it has some drawbacks such as hysteresis behavior, drift in time, temperature dependence and vibration effects. Molecular friction at sites of materials imperfections due to domain walls motion is the general cause of hysteresis in piezoelectric materials [3]. The hysteresis is a major nonlinearity for piezo-actuators and often limits system performance via undesirable oscillations or instability. Therefore, it is difficult to obtain an accurate trajectory tracking control. Numerous mathematical methods have been proposed to analyze the hysteresis behavior of piezoelectric actuators. These studies may be categorized in asymmetrical and symmetrical methods. The asymmetrical types of hysteretic models include polynomial model [4], Preisach's model [5], neural network model [6] and Karasnoselskii and Pokrovskii [7]. The symmetrical types of hysteretic model include Duhem model [8], Bouc-Wen model [9] and Lugre model [9].

The asymmetrical methods establish the nonlinear relations between the input and output based on the measured input/output data sets. Because superposition of a basic hysteresis operator is a fundamental principle in these models, they are also called to operator based model. Although, an operator based model may give a good match with experimental data, the dynamics of the piezoelectric material is not formulated in these modeling methods and model parameter identification and implementation is more difficult in this case. The symmetrical methods employ nonlinear differential equations in order to describe hysteresis. In this case, the dynamics of the piezoelectric materials are described but the non-symmetric hysteresis is not modeled. However these models are more tractable for control design. In order to include the hysteresis effect and compensating its effect, Lugre model [10] is analyzed and studied in this chapter.

There are several control methods to overcome the above mentioned errors and increase the tracking control precision of the piezoelectric actuators. Some of these methods are PI and PID controller, fuzzy controller [11], adaptive RFNN [12], feed-forward model reference control method [13], adaptive hysteresis inverse cascade with the plant [14], reinforcement discrete neuro-adaptive controller [15], adaptive wavelet neural network controller [16], nonlinear observer-based sliding-mode controller [17] an adaptive backstepping controller [10, 18], robust motion tracking controller based on sliding-mode theory [19] and continuous time controller based on SMC and disturbance observer [20]. In some of these works, a complex inverse hysteresis model has been adopted to overcome the nonlinear hysteresis effect. Also, in the methods based on the neural network approach, to ensure the error is bounded, it is assumed that the system states must be inside a compact set. Moreover, robustness against parameters uncertainties and external disturbances is the other problem encounter the control methods presented for piezoelectric actuator.

In this chapter, a robust motion tracking control strategy in combination with the hysteresis force observer is designed and investigated for the piezoelectric actuator. The presented controller is robust against the unknown or uncertain system parameters and can estimate the hysteresis force with its estimation property. This control strategy is established based on the lumped parameter dynamic model. Using Lyapanouv stability analysis, the stability analysis of the overall control and observer system is performed. Furthermore, the validity and effectiveness of the designed methodology is investigated by numerical analysis and its results obtained are compared with those of [19].

Section 2 contains the model explanation of piezo-positioning mechanism. A hysteresis model for piezoelectric systems based on Lugre model is discussed in section 3. Design procedure of the developed controller is presented in section 4. Simulation analysis and results obtained are presented in section 5. Finally, section 6 includes the conclusion of this chapter.

2. Model of piezo-positioning mechanism with hysteresis

The lumped parameter dynamic model of the piezo-driven mechanism is written as [10, 16]:

$$M\ddot{x} + D\dot{x} + F_H + F_L = u \tag{1}$$

Where M is the mass of the controlled piezo-positioning mechanism, D is the linear friction coefficient of the piezo-driven system, F_L denotes the external load, F_H is the hysteresis friction force function, $x(t), \dot{x}(t)$, and $\ddot{x}(t)$ denote the piezoelectric displacement, velocity and acceleration, respectively and u is the applied voltage to the piezo-positioning mechanism.

A block diagram of the model (1) is depicted in Fig.1. Note that the simulation program used in this chapter is C++.

Noted that:

$$\left|F_H(t)\right| \le \delta F_{H0}\,, \left|\dot{F}_H(t)\right| \le \delta F_{H1}\,, \left|\ddot{F}_H(t)\right| \le \delta F_{H2}\,,, \left|F_L(t)\right| \le \delta F_{L0}\ \left|\dot{F}_L(t)\right| \le \delta F_{L1}\,, \left|\ddot{F}_L(t)\right| \le \delta F_{L2} \tag{2}$$

Where $\delta F_{Hi} \in \Re^1, i = 0,1,2$ and $\delta F_{Li} \in \Re^1, i = 0,1,2$ denote the known upper bounds.

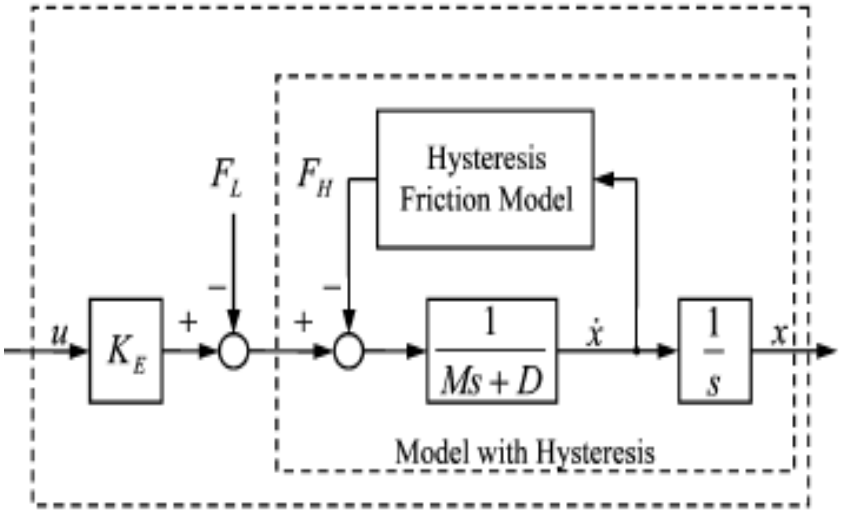

Fig. 1. Model of piezo-positioning mechanism with hysteresis [10].

3. Lugre hysteresis model for piezo-positioning system

This chapter uses Lugre model to describe nonlinear hysteretic curve of piezoelectric systems. The mathematical equation is as follows [10,16]:

$$F_H = \sigma_0 z - \sigma_1 \frac{1}{g(\dot{x})} z|\dot{x}| + (\sigma_1 + \sigma_2)\dot{x} \tag{3}$$

$$\dot{z} = \dot{x} - \frac{|\dot{x}|}{g(\dot{x})} z \tag{4}$$

Where z interpreted as the contact force applied voltage average bristle coefficient, $\sigma_0, \sigma_1, \sigma_2$ are positive constants and generally can be equivalently interpreted a bristle stiffness, damping and viscous-damping coefficients, respectively. Moreover, the function $g(\dot{x})$ denotes the Stribeck effect curve described by:

$$\sigma_0 g(\dot{x}) = f_C + (f_S - f_C) e^{-(\dot{x}/\dot{x}_S)^2} \tag{5}$$

Where f_C is the coloumb friction level, f_S is the level of stiction force and $\dot{x}_S$ is the Stribeck velocity. The function $g(\dot{x})$ is positive and constant [16]. As depicted in [10], the following lemma is held.

Lemma 1. Consider nonlinear dynamics system of (4). For any piecewise continuous signal x and $\dot{x}$, the output $z(t)$ is bounded.

Substituting the (3) in (1) and arranging the expression, the following dynamics equation is obtained for the piezo-positioning mechanism with Lugre hysteresis model:

$$\ddot{x} = \frac{1}{M}u - \frac{1}{M}\left[(\sigma_0 z + F_L) - \sigma_1 \frac{z|\dot{x}|}{g(\dot{x})} + (\sigma_1 + \sigma_2)\dot{x} \right] - \frac{D}{M}\dot{x} \tag{6}$$

4. Design controller

In this section we design a robust control strategy for the system of (1), to asymptotically estimate the hysteresis parameter of equation (3). To facilitate the design process, we assumed that the hysteresis force is dependent only on the time and F_H and its first two time derivatives remain bounded for all times. Using (6) we can rewrite equation (1) as:

$$\ddot{x} = \frac{u}{M} - \frac{F}{M} - \frac{D}{M}\dot{x} \tag{7}$$

Where $F = (\sigma_0 z + F_L) - \sigma_1 \frac{z|\dot{x}|}{g(\dot{x})} + (\sigma_1 + \sigma_2)\dot{x}$ is a combination of an unknown friction hysteresis force function and external load, which must be estimated.

The dynamics of a piezo-positioning system can be represented by the following equation:

$$\bar{M}\ddot{x} + \bar{D}\dot{x} + F - u + (\Delta M\ddot{x} + \Delta D\dot{x}) = 0 \tag{8}$$

Where $\bar{M}$ and $\bar{D}$ are the nominal parameter values of the mass and linear friction coefficient and ΔM and ΔD are the parametric errors between real value and nominal value of the uncertain parameters of the system and modeled as:

$$|\Delta M| \le \delta M \tag{9}$$

$$|\Delta D| \le \delta D \tag{10}$$

Where δM and δD are the bounds of system parameters. The position tracking error signal is defined as:

$$e = x_d - x \tag{11}$$

Where $x_d \in \Re^1$ denotes the desired position trajectory. The desired piezo-position trajectory and its first three time derivatives are assumed to be constrained by the following:

$$|x_d| < \zeta_{d0}, |\dot{x}_d| < \zeta_{d1}, |\ddot{x}_d| < \zeta_{d2}, |\dddot{x}_d| < \zeta_{d3} \tag{12}$$

Where the ζ_{di}'s denote known positive constants. Also, the filtered tracking error signal $r(t) \in \Re^1$ is defined as:

$$r = \dot{e} + \alpha e \tag{13}$$

Where $\alpha \in \Re^1$ is a positive constant control gain.

The system dynamics of (8) are rewritten in terms of the filtered tracking error signal $r(t)$ as follows:

$$\dot{r} = (\ddot{x}_d + \alpha\dot{e}) + \frac{\bar{D}}{\bar{M}}\dot{x} + \frac{F}{\bar{M}} + \frac{1}{\bar{M}}(\Delta M\ddot{x} + \Delta D\dot{x}) - \frac{u}{\bar{M}} \tag{14}$$

We define χ as:

$$\chi = \frac{1}{\bar{M}}(\Delta M\ddot{x} + \Delta D\dot{x}) \le \frac{1}{\bar{M}}(\delta M|\ddot{x}| + \delta D|\dot{x}|) = \frac{1}{\bar{M}}\beta_1(x) \tag{15}$$

Another filtered tracking error signal $s(t) \in \Re^1$ is defined as:

$$s = \dot{r} + \beta r \tag{16}$$

Where β is a constant positive parameter.

Based on the developed error system and ensuring the stability analysis, the following control input signal for the system (14) is designed:

$$u = \bar{M}(\ddot{x}_d + \alpha\dot{e}) + \bar{D}\dot{x} + \hat{F} + \beta_1(x)\mathrm{sgn}(s) \tag{17}$$

Where $\hat{F} \in \Re^1$ represents the estimation of F and is obtained by the following observer:

$$\dot{\hat{F}} = -(k_1 + \beta)\hat{F} + k_1\beta r + \rho\,\mathrm{sgn}(r) \tag{18}$$

Where sgn(.) is the standard signum function, and $k_1, \rho \in \Re^1$ are positive constants.

Noted that the equation (18) for $\hat{F}$ is a stable linear system with the disturbance term $k_1\beta r + \rho\,\mathrm{sgn}(r)$.

To facilitate the dynamic system stability analysis, the auxiliary disturbance signal $\eta(t) \in \Re^1$ is defined by:

$$\eta = \dot{F} + (k_1 + \beta)F \tag{19}$$

Due to the boundness of F and its first two time derivatives, it is understand that $\eta(t), \dot{\eta}(t) \in L_\infty$.

Based on the stability analysis, the constant ρ should be chosen to satisfy the following inequality:

$$\rho \ge |\eta(t)| + \frac{1}{\beta}|\dot{\eta}(t)| \tag{20}$$

By substituting (17) in (14), and simplify the obtained expression, the dynamics of $\dot{r}$ is achieved as:

$$\dot{r} = F - \hat{F} + \frac{1}{\bar{M}}(\chi_1(x) - \beta_1(x)\mathrm{sgn}(s)) \tag{21}$$

Where $\chi_1(x) = \Delta M\ddot{x} + \Delta D\dot{x}$.

Now, using (21), the time derivative of (16) is obtained as:

$$\dot{s} = \dot{F} - \dot{\hat{F}} + \frac{1}{\bar{M}}(\dot{\chi}_1(x) - \dot{\beta}_1(x)\mathrm{sgn}(s)) + \beta(F - \hat{F} + \frac{1}{\bar{M}}(\chi_1(x) - \beta_1(x)\mathrm{sgn}(s))) \tag{22}$$

Substituting (18) and (19) in (22), gives:

$$\dot{s} = \eta - k_1 s - \rho\,\mathrm{sgn}(r) + \frac{1}{\bar{M}}(\dot{\chi}_1(x) - \dot{\beta}_1(x)\mathrm{sgn}(s)) + \frac{\beta + k_1}{\bar{M}}(\chi_1(x) - \beta_1(x)\mathrm{sgn}(s)) \tag{23}$$

Remark 1: If $s(t) \in L_\infty$, then $r(t), \dot{r}(t) \in L_\infty$ and if $s(t)$ is asymptotically regulated, then $r(t), \dot{r}(t)$ are also, asymptotically regulated.

5. Stability analysis

Theorem 1. For the dynamics of (7), the designed controller of (17) and (18) guarantees the global asymptotetic piezo-driven position tracking in the sense that:

$$\lim_{t\to\infty} e(t) = 0 \tag{24}$$

And global asymptotetic estimation of hysteresis in the sense that:

$$\lim_{t\to\infty}[\hat{F} - F] = 0 \tag{25}$$

With the constant ρ satisfies the condition of (20).

Proof

A non-negative, scalar function $V(t) \in \Re^1$ is defined as:

$$V = \frac{1}{2}s^2 \tag{26}$$

Tacking time derivative of (26) gives:

$$\dot{V} = -k_1 s^2 + (\dot{r} + \beta r)(\eta - \rho\,\mathrm{sgn}(r)) + \frac{s}{\bar{M}}(\dot{\chi}_1(x) - \dot{\beta}_1(x)\mathrm{sgn}(s)) + \frac{\beta + k_1}{\bar{M}} s(\chi_1(x) - \beta_1(x)\mathrm{sgn}(s)) \tag{27}$$

From (15) it is clear that:

$$\frac{1}{\bar{M}}(\dot{\chi}_1(x) - \dot{\beta}_1(x)\mathrm{sgn}(s)) + \frac{\beta + k_1}{\bar{M}}(\chi_1(x) - \beta_1(x)\mathrm{sgn}(s)) \le 0 \tag{28}$$

Where $\dot{\beta}_1(x) = \delta M|\ddot{x}| + \delta D|\ddot{x}|$.

Hence:

$$\dot{V} \le -k_1 s^2 + (\dot{r} + \beta r)(\eta - \rho\,\mathrm{sgn}(r)) \tag{29}$$

After integrating both sides of (29), the following inequality is obtained:

$$V(t)-V(t_0)\le -k_1\int_{t_0}^{t}s^2(\sigma)d\sigma+\left[|r(t)||\eta(t)|-\rho|r(t)|\right]+\left[\int_{t_0}^{t}\beta|r(\sigma)|\left(|\eta|+\frac{1}{\beta}\left|\frac{d\eta(\sigma)}{d\sigma}\right|-\rho\right)d\sigma\right]+\zeta_0 \quad (30)$$

Where $\zeta_0\in\Re^1$ is a positive constant, defined by:

$$\zeta_0=|r(t_0)||\eta(t_0)|+\rho|r(t_0)| \quad (31)$$

After applying the (20) to the bracketed term of (30), $V(t)$ can be upper bounded as follows:

$$V(t)\le V(t_0)-k_1\int_{t_0}^{t}s^2(\sigma)d\sigma+\zeta_0 \quad (32)$$

It is deduced from (32) and (26) that $V(t)\in L_\infty$ and $s(t)\in L_\infty$, respectively. Finally utilizing remark 1, $r(t),\dot{r}(t),e(t),\dot{e}(t),\dot{s}(t)\in L_\infty$.

Equation (32) rearrange as:

$$k_1\int_{t_0}^{t}s^2(\sigma)d\sigma\le V(t_0)-V(t)+\zeta_0 \quad (33)$$

From the fact that $V(t)$ is non-negative and equation (33), it can be deduced that $s(t)\in L_2$. Because of $s(t)\in L_\infty\cap L_2$ and $\dot{s}(t)\in L_\infty$, we can use the Barbalat's Lemma [21] to summarized that:

$$\lim_{t\to\infty}s(t)=0 \quad (34)$$

Therefore:

$$\lim_{t\to\infty}r(t),\dot{r}(t),e(t),\dot{e}(t)=0 \quad (35)$$

6. Simulation results

In this section, simulation results are presented to investigate the performance of the presented method for piezoelectric actuator. First, we test the controller response with the nominal value of piezoelectric actuator, when $F_L=0.3\sin(t)$ and initial values are: $x(0)=0,\dot{x}(0)=0,z(0)=0$. The objective of the positioning is to drive the displacement signal x to track the reference trajectory which is shown in Fig.2.

The parameters of piezo-positioning mechanism are given in Table 1.

$\sigma_0=50000N/m$	$\sigma_1=\sqrt{5\times10^4}Ns/m$	$\sigma_2=0.4Ns/m$
$f_C=1N$	$f_S=1.5N$	$\dot{x}_S=0.001m/s$
$M=1kg$	$D=0.0015Ns/m$	$F_L=0.3\sin(t)$

Table 1. Piezoelectric Parameters

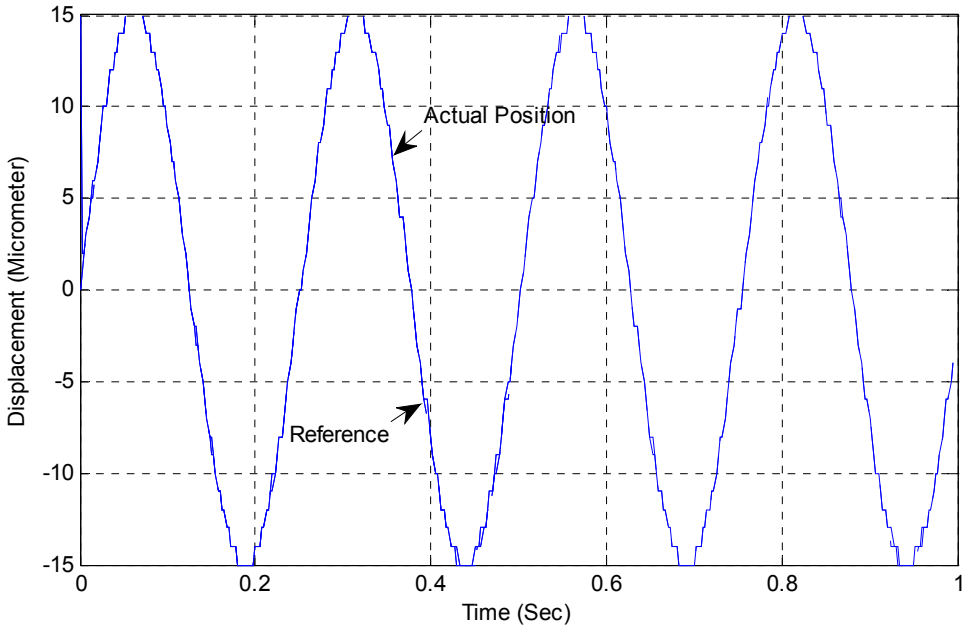

Fig. 2. Desired and Actual Piezoelectric displacement.

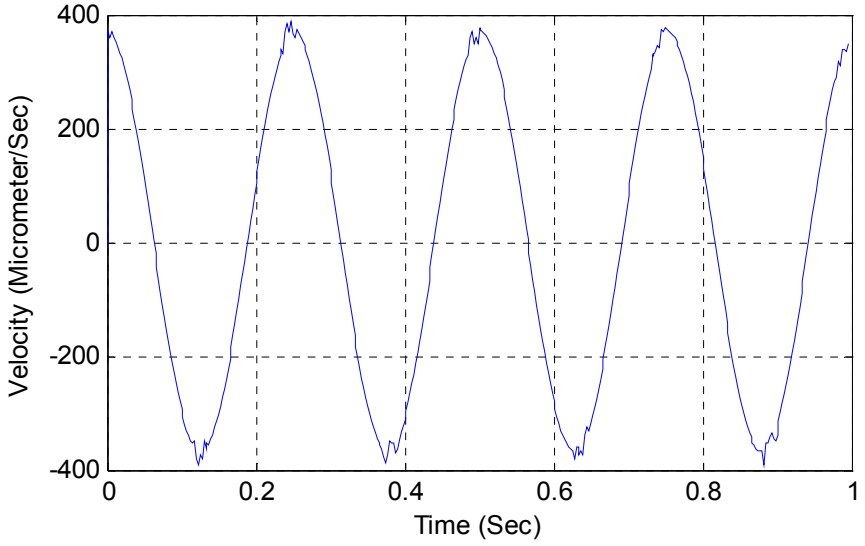

Fig. 3. Piezoelectric velocity.

As depicted from the results, especially Fig.4, the positioning mechanism has a good accuracy and the error between displacement and reference signal at least 4 orders is smaller than the actual signal which means that the error is about %0.01.

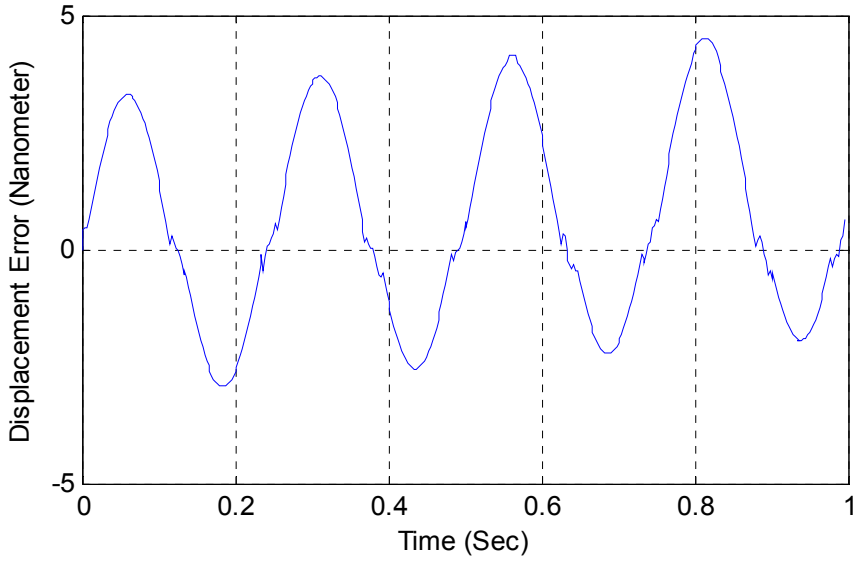

Fig. 4. Error between actual & desired displacement.

For the purpose of study the behavior of the controller in the presence of parameter uncertainties, by considering the $\Delta M = 0.1\bar{M}$, $\Delta D = 0.1\bar{D}$ and $\Delta F_L = 0.4$ and using $x(0) = 15(\mu m), \dot{x}(0) = 0, z(0) = 0$ as the initial values, we have performed another test. The result of this test is compared with the result of the method presented in [19]. In the simulation we consider the control gain α is 2000.

As it can be seen from Fig.5 and Fig.7, the presented method has an acceptable response and the positioning error is in about %0.25. Also, the hysteresis and disturbance voltage and its estimation are shown in Fig.9. As it can be seen from this result, the hysteresis identifier can estimate the hysteresis voltage precisely. For the purpose of comparison the accuracy of the proposed method with the recently proposed method in [19], we simulate the piezo-positioning mechanism with the method of [19]. The displacement error of [19] is shown in Fig.10. Noted that in the simulation of [19] we use these control gains: $k_p = 10^5, k_v = 9000, k_s = 50$ and $\alpha = 10$. Comparison of Fig.7 and Fig.10 depicts that the error in the presented method is smaller than the method of [19]. Also, it is clear that in addition of smaller number of control gains, the gain of the controller in the presented method in comparison with [19] is very smaller. Experimental implementation of the high gain needs more complexity and also it may be generate noise. Although method of [19] is

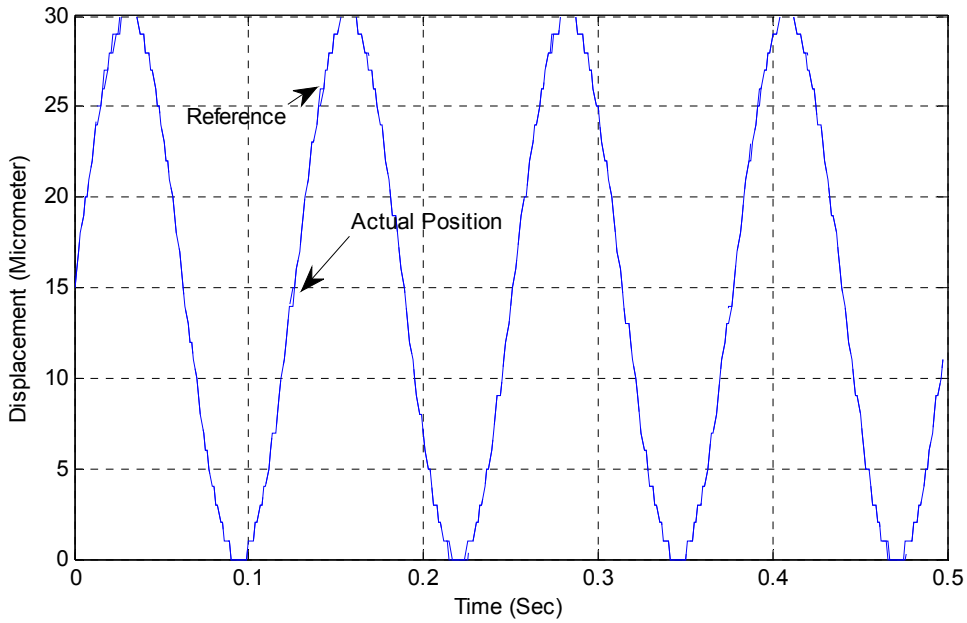

Fig. 5. Displacement of piezoelectric.

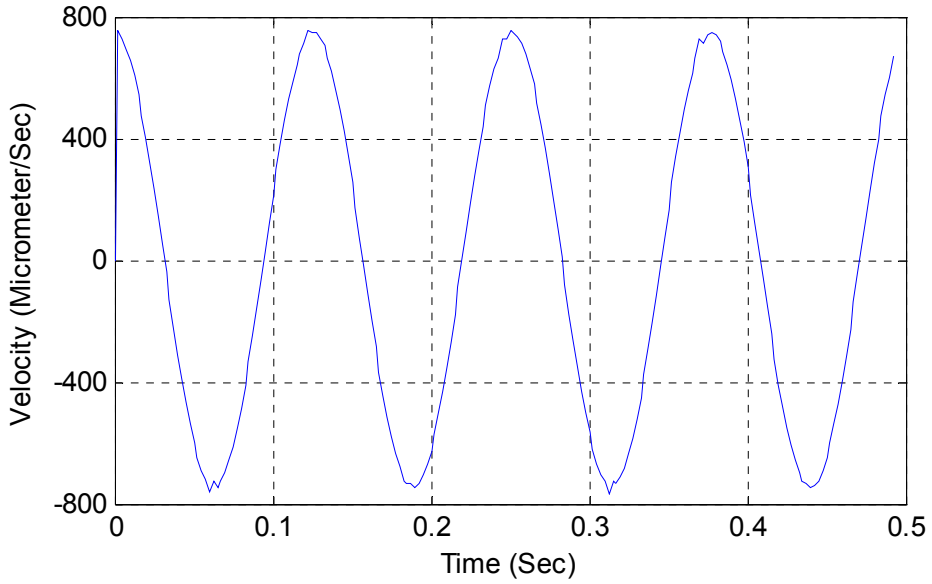

Fig. 6. Velocity of piezoelectric.

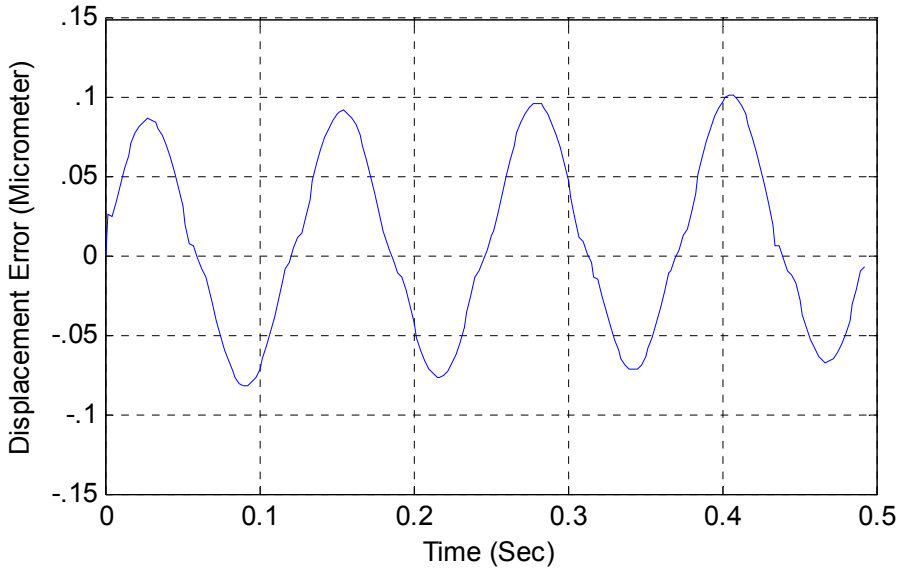

Fig. 7. Error between actual & desired displacement.

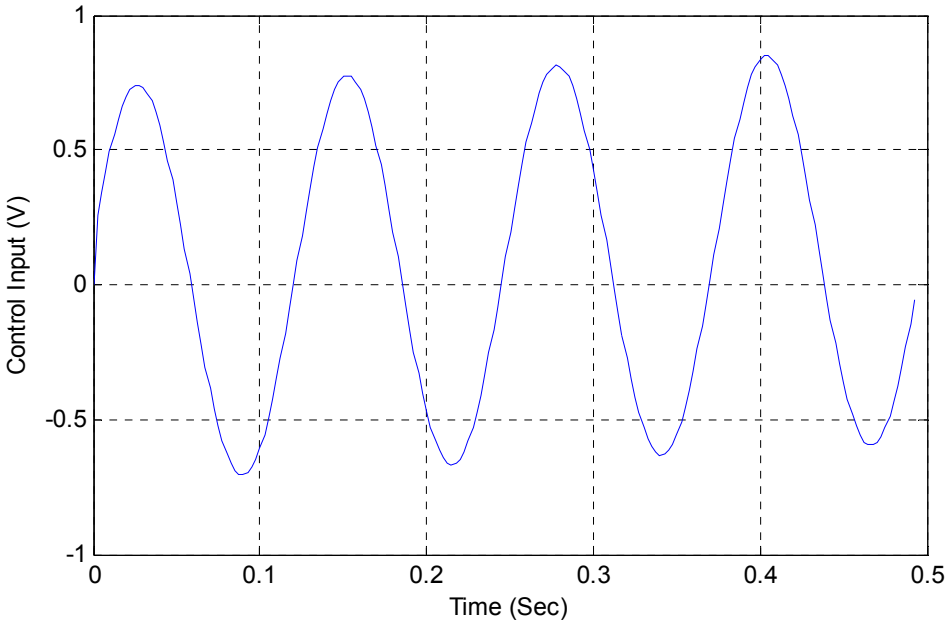

Fig. 8. Control input.

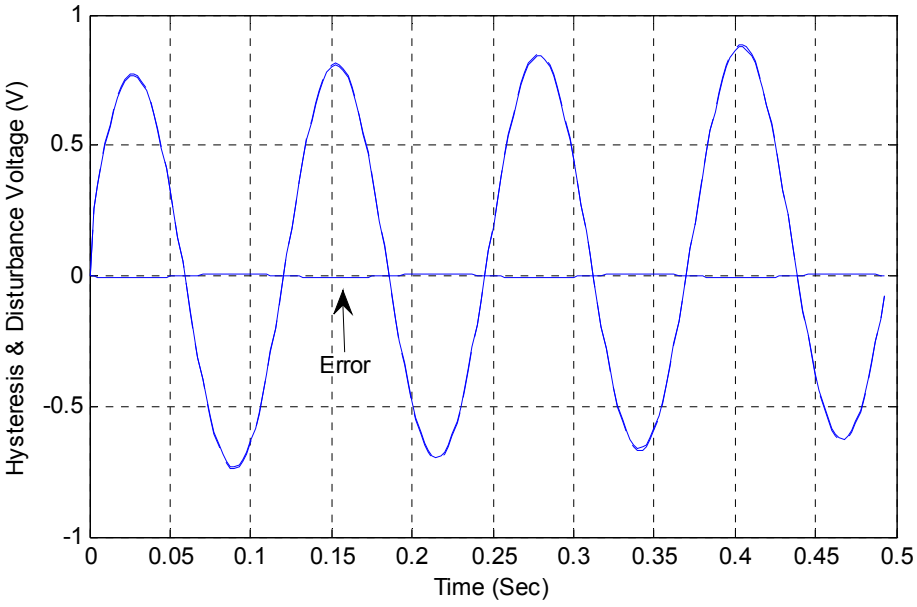

Fig. 9. Estimated & actual values of hysteresis and disturbance voltages and error between them.

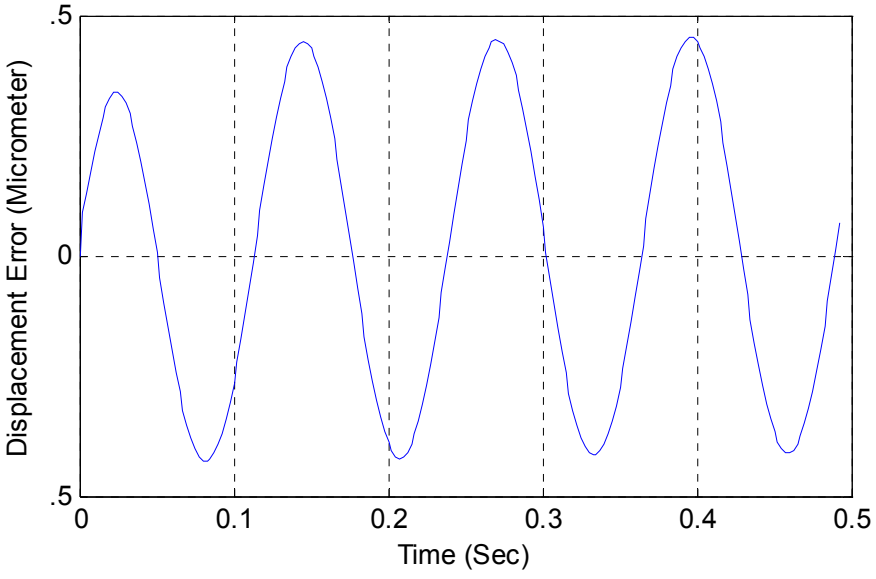

Fig. 10. Displacement Error of the method presented in [19].

robust against disturbances and uncertainties and in comparison with other methods has higher precision, it needs high value gains to perform this task. While the proposed method can perform these tasks with lower cost and also it has the capability of hysteresis estimation.

For the comparison between the presented method and the method of [19] another simulation test is carried out. In this case $\Delta M = 0.2\bar{M}$, $\Delta D = 0.2\bar{D}$ and $\Delta F_L = 0.4$. The result is shown in Fig.11.

As it can be depicted the presented method has the better response and using the proposed controller the error is decreased. Note that in this case the reference is similar to the Fig.5.

The last simulation is devoted to the reference signal of Fig.2 by considering $\Delta M = 0.2\bar{M}$, $\Delta D = 0.2\bar{D}$ and $\Delta F_L = 0.4$. Also in this case the error of the proposed controller is less than the method of [19].

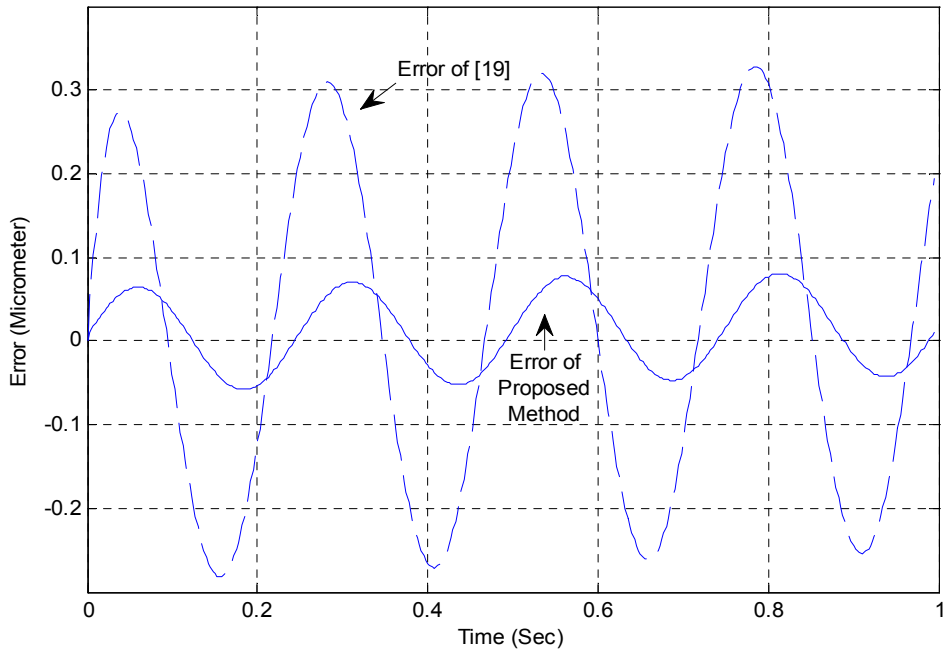

Fig. 11. Comparison between the displacement error of the presented controller and the controller proposed in [19].

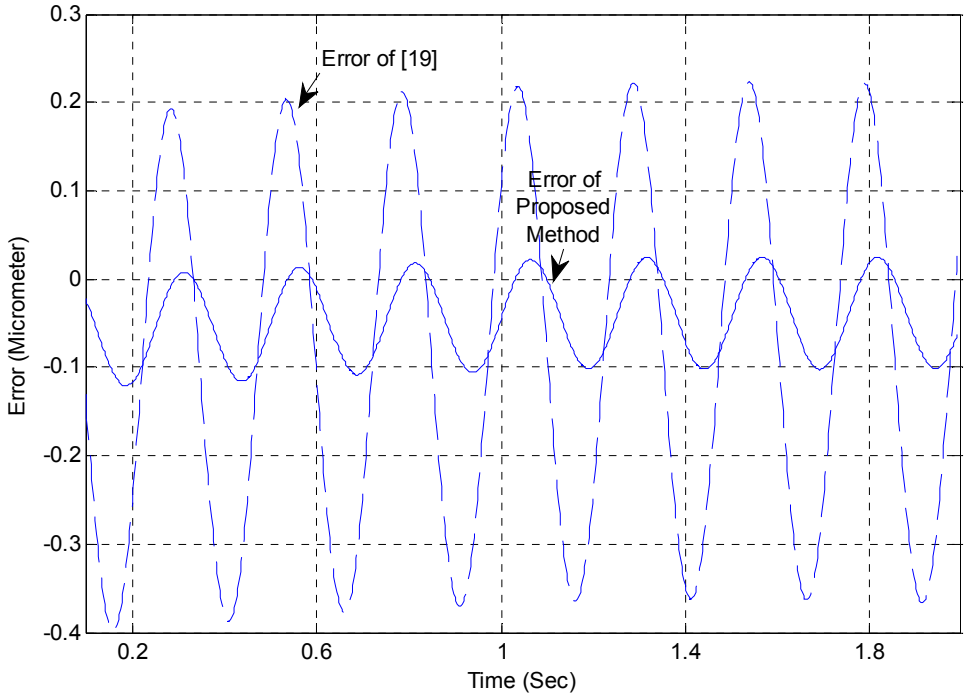

Fig. 12. Comparison between the displacement error of the presented controller and the controller proposed in [19].

7. Conclusion

A robust tracking motion controller is designed to control a positioning of piezoelectric actuator system with hysteresis phenomenon. The Lugre hysteresis model is used to model the nonlinearities in the system under study. Using the presented controller, we can estimate the nonlinear hysteresis and disturbances imposed to the piezoelectric actuator and compensate their effects. The performance and efficiency of the designed controller for a positioning system is compared with recently proposed robust method. The results obtained depict the validity and performance of the presented approach.

8. References

[1] Spanner, K. and S. Vorndran, 2003. Advances in piezo-nanopositioning technology. Proc. IEEE/ASME int. conf. advanced intelligent mechatronics, Kobe, Japan.

[2] Yi B.J., G.B. Chung, H.Y. Na, W.K. Kim and I.H. Suh, 2003. Design and experiment of a 3-DOF parallel micromechanism utilizing flexurehinges. IEEE Trans Robotics Automation, 19(4): 604–12.

[3] EI Rifai, O.M., 2002. Modeling and control of undesirable dynamics in atomic force microscopes. PhD dissertation, MIT, February.

[4] Hung, X.C. and D.Y. Lin, 2003. Tracking control of a piezoelectric actuator based on experiment hysteretic modeling. Proc. Of the IEEE/ASME Int. Conf. Advanced Intelligent Mechatronics, Kobe, Japan.

[5] Ge, P. and M. Jouaneh, 1997. Generalized priesach model for hysteresis nonlinearity of piezoceramic actuators. Precision Eng., 20: 99-111.

[6] Richter, H., E.A. Misawa, D.A. Lucca and H. Lu, 2001. Modeling nonlinear behavior in a piezoelectric actuator. Prec. Eng. J., 25: 128-137.

[7] Krasnosellskii, M.A. and A.V. Pokrovskii, 1989. Systems with hysteresis, Springer-Verlag, Berlin.

[8] Stepanenko, Y. and C.Y. Su, 1998. Intelligent control of piezoelectric actuators. Proc. IEEE Conf. Decision & Control, 4234-4239.

[9] Wen, Y.K. 1976. Method for random vibration of hysteresis system. J. Eng. Mechanics Division, 102: 249-263.

[10] Zhou, J., C. Wen and C. Zhang, 2007. Adaptive backstepping control of piezo-positioning mechanism with hysteresis. Trans. CSME, 31(1): 97-110.

[11] Yavari, F., M.J. Mahjoob, and C. Lucas, 2007. Fuzzy control of piezoelectric actuators with hysteresis for nanopositioning. 13th IEEE/IFAC Int. Conf. on Methods and Models in Automation and Robotics, 685-690, August.

[12] Xu, J.H. 1993. Neural network control of a piezo tool positioner. Canadian Conf. Elect. & Comp. Eng., 1: 333-336.

[13] Jung, S.B. and S.W. Kim, 1994. Improvement of scanning accuracy of pzt piezoelectric actuator by feed-forward model-reference control. Precision Engineering, 16: 49-55.

[14] Tao, G. and P.V. Koktokovic, 1995. Adaptive control of plants with unknown hysteresis. IEEE Transaction on Auotomatic Control, 40: 200-212.

[15] Huwang, L. and C. Jans, 2003. A reinforcement discrete neuro-adaptive control of unknown piezoelectric actuator systems with dominant hysteresis. IEEE Trans. Neural Networks, 14: 66-78.

[16] Lin, F.J., H.J. Shieh, and P.K. Huang, 2006. Adaptive wavelet neural network control with hystereis estimation for piezo-positioning mechanism. IEEE Trans. Neural Networks, 17: 432-444.

[17] Jan, C. and C.L. Hwang, 2004. A nonlinear observer-based sliding-mode control for piezoelectric actuator systems: theory and experiments. J Chinese Inst. Eng.,27(1): 9-22.

[18] Shieh H.J., F.J. Lin, P.K. Huang, and L.T. Teng, 2004. Adaptive tracking control solely using displacement feedback for a piezo-positioning mechanism. IEE Proc Control Theory Appl,151(5): 653–60.

[19] Liaw, H.C., B. Shirinzadeh, and J. Smith, 2008. Robust motion traking control of piezo-driven flexure-based four bar mehanism for micro/nano manipulation. Mechatronics, 18: 111-120.

[20] Yannier, S. and A. Sabanovic, 2007. Continuous Time Controller Based on SMC and Disturbance Observer for Piezoelectric Actuators. Int. Rev. Elect. Eng (I.R.E.E.), 3 (6).

[21] Spooner, J.T., M. Maggiore, R. Ordonez, and K.M. Passino, 2002. Stable Adaptive Control and Estimation for Nonlinear Systems. John Wiley and Sons, Inc, NY.

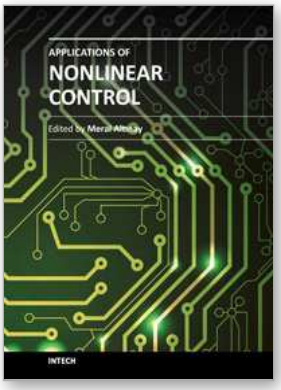

Applications of Nonlinear Control

Edited by Dr. Meral Altınay

ISBN 978-953-51-0656-2
Hard cover, 202 pages
Publisher InTech
Published online 13, June, 2012
Published in print edition June, 2012

A trend of inverstigation of Nonlinear Control Systems has been present over the last few decades. As a result the methods for its analysis and design have improved rapidly. This book includes nonlinear design topics such as Feedback Linearization, Lyapunov Based Control, Adaptive Control, Optimal Control and Robust Control. All chapters discuss different applications that are basically independent of each other. The book will provide the reader with information on modern control techniques and results which cover a very wide application area. Each chapter attempts to demonstrate how one would apply these techniques to real-world systems through both simulations and experimental settings.

How to reference

In order to correctly reference this scholarly work, feel free to copy and paste the following:

Amir Farrokh Payam, Mohammad Javad Yazdanpanah and Morteza Fathipour (2012). A Robust Motion Tracking Control of Piezo-Positioning Mechanism with Hysteresis Estimation, Applications of Nonlinear Control, Dr. Meral Altınay (Ed.), ISBN: 978-953-51-0656-2, InTech, Available from: http://www.intechopen.com/books/applications-of-nonlinear-control/a-robust-motion-tracking-control-of-piezo-positioning-mechanism-with-hysteresis-estimation

INTECH
open science | open minds

InTech Europe
University Campus STeP Ri
Slavka Krautzeka 83/A
51000 Rijeka, Croatia
Phone: +385 (51) 770 447
Fax: +385 (51) 686 166
www.intechopen.com

InTech China
Unit 405, Office Block, Hotel Equatorial Shanghai
No.65, Yan An Road (West), Shanghai, 200040, China
中国上海市延安西路65号上海国际贵都大饭店办公楼405单元
Phone: +86-21-62489820
Fax: +86-21-62489821